PERGAMON

Vision Research 39 (1999) 3071–3081

Vision Research

www.elsevier.com/locate/visres

Section 3

The visual physiology of the wild type mouse determined with pattern VEPs

Vittorio Porciatti [a,*], Tommaso Pizzorusso [b], Lamberto Maffei [a,b]

[a] *Istituto di Neurofisiologia del CNR, 51, Via San Zeno, 56127 Pisa, Italy*
[b] *Scuola Normale Superiore, 56127 Pisa, Italy*

Received 13 October 1998; received in revised form 21 December 1998

Abstract

Genetically manipulated mice are important tools for studies on plasticity and degeneration/regeneration in the visual system. However, a description of the basic properties of the visual performance of the wild type mouse is still lacking. To characterize the visual physiology of the wild type (C57BL/6J) mouse we recorded Visual Evoked Potentials (VEPs) from the primary visual cortex. As compared to behavioral methods, VEPs may have the advantage that different aspects of vision can be screened readily and simultaneously in the same animals, including those with poor visual behavior due to motor or learning deficits. Local VEP responses to patterned visual stimuli have been recorded from the binocular visual cortex of anesthetized mice. Spatial (visual acuity, contrast threshold) and temporal (temporal function, response latency, motion sensitivity) aspects of VEPs were evaluated. The mouse VEP acuity was 0.6 c/deg, which is comparable to the behavioral visual acuity. The VEP peak contrast threshold was 5% (no behavioral data are available). Cortical representation of visual coordinates and cortical magnification factor corresponded to those previously reported using single cell recordings. Laminar analysis of VEPs indicated a dipole source in the supragranular layers of the visual cortex as a major response generator. VEPs showed contribution from both eyes, although biased strongly towards the eye contralateral to the recorded cortex. Results provide a comprehensive framework for characterizing visual phenotypes of a variety of transgenic mice.

Keywords: Mouse; Visual cortex; Visual evoked potentials; Patterned visual stimuli

1. Introduction

The mammalian visual system has been the traditional target for studies of developmental plasticity (Katz & Shatz, 1996) and degeneration/regeneration (Aguayo, Rasminsky, Bray, Carbonetto, McKerracher, Villegas-Perez et al., 1991). This research could gain great advantage from the use of a number of mouse mutants introduced by the modern techniques of molecular biology (Silva, Simpson, Takahashi, Lipp, Nakanishi, Wehner et al., 1997). Unfortunately, the knowledge of mouse vision is scanty (Fuller & Wimer, 1966; Sinex, Burdette & Pearlman, 1979). This sets a severe limit for the evaluation of the effects induced by experimental manipulations. The present study addresses the issue of the mouse visual physiology by means of visual evoked potentials (VEPs) recorded from specific regions of the binocular visual cortex in response to visual patterns modulated in space and time. Pattern VEPs may provide a comprehensive framework for characterizing visual phenotypes of a variety of transgenic mice. As compared to behavioral methods, VEPs may have the advantage that different aspects of vision can be tested simultaneously in the same animals, including those with poor visual behavior due to motor or learning deficits (Crawley & Paylor, 1997; Post & Weiss, 1997). VEPs have been used on one hand to obtain a measure of visual capabilities (spatial resolution, contrast threshold, response timing) which have a counterpart in behavioral capabilities (visual

* Corresponding author. Tel.: +39-50-540770; fax: +39-50-540080.
E-mail address: porciatt@in.pi.cnr.it (V. Porciatti)

0042-6989/99/$ - see front matter
PII: S0042-6989(99)00022-X

acuity, contrast sensitivity, reaction time), and on the other hand to obtain information on local cortical processing (cortical retinotopy, laminar analysis). A further aim of this study was to establish the relative contribution of either eye to the VEPs. Preliminary results have been previously published in abstract form (Pizzorusso, Porciatti, Strettoi & Maffei, 1997).

2. Materials and methods

2.1. Electrophysiology

A total of 28 C57B7L/6J mice of both sexes (Charles River) 2–3 months old have been used. Mice were anesthetized with an intraperitoneal injection of 20% urethane (Sigma, 8 ml/kg) and mounted in a stereotaxic apparatus allowing full viewing of the visual stimulus. Eyes were not restrained in a fixed position, nor eyelids were kept artificially opened. The pupil was not dilated and was always clearly observable between eyelid margins. At the end of the recording session the pupil was dilated with 2.5% phenylephrine hydrochloride and 1% tropicamide to check that the eye optics was transparent (Fraunfelder & Burns, 1970) and in some cases to project the optic disk on a tangent screen positioned at the same distance as the visual stimulator. In agreement with previous reports (Drager, 1975; Wagor, Mangini & Pearlman, 1980; Gordon & Stryker, 1996) we found that optic disk location is very stable among animals. Eyes were not refracted. It is known that the mouse eye is emmetropic and with large depth of focus due to the pinhole pupil (Remtulla & Hallet, 1985). In addition, previous work recording the pattern electroretinogram (Porciatti, Pizzorusso, Cenni & Maffei, 1996) and present controls recording VEPs, indicated that responses are not modified by trial lenses (± 10 D in power) placed before the eye. Body temperature was monitored with a rectal probe and maintained at 37.0°C with a heating pad. A large portion of the skull (4×4 mm) overlying the binocular visual cortex was carefully drilled and removed leaving the dura intact. A resin-coated microlectrode (WPI, Sarasota) with tip impedance of 0.5 MΩ was inserted into the cortex perpendicularly to the stereotaxic plane. Due to curvature of the brain surface, the electrode track formed and angle of approximately 30° with the line perpendicular to cortical surface. In most experiments, microelectrodes were inserted 2.6–3.2 mm lateral to the lambda (intersection between sagittal- and lambdoid-sutures), and advanced 400 μm within the cortex. At that depth VEPs had their maximal amplitude. The region of the visual field yielding VEPs of maximal amplitude was established for each penetration, by recording a series of responses to stimuli windowed to either a vertical or horizontal stripe of $10 \times 86°$ and presented at several different visual field azimuths and elevations, respectively. A window size of 10° was chosen as a compromise between VEP amplitude and spatial selectivity. Spatial integration of the microelectrode was inferred by the VEP amplitude dependence on window size. Typically, VEP amplitude reaches about 80% of its maximum with a 10° window and saturates for a window of about 20° (not shown in figures). In experiments of laminar analysis, microelectrodes were advanced 50–1000 μm in 50 μm steps within the cortex and the electrode track was reconstructed by electrolytic lesions (5 μA, 5 s) made at several cortical depths. Electrical signals were amplified (50 000 fold), band-pass filtered (0.3–100 Hz, -6 dB/oct), digitized (12 bit resolution) and averaged (at least 128 events in blocks of 16 events each) in synchrony with the stimulus contrast reversal. Transient VEPs in response to abrupt contrast reversal (1 Hz) were evaluated in the time domain by measuring the peak-to-trough amplitude and peak latency of the major component (see below). Steady-state VEPs in response to sinusoidal modulation of contrast at different temporal frequencies were evaluated in the frequency domain by measuring the amplitude and phase of the major response component (second harmonic). Partial averages contributing to the total average were used to calculate response reliability (standard error of amplitude variation). VEPs in response to an occluded stimulus were also frequently recorded to have an estimate of the residual noise.

2.2. Visual stimuli

Typical visual stimuli were horizontal sinusoidal gratings of different spatial frequency and contrast generated by a VSG2/2 card (Cambridge Research System, Cheshire, UK) and presented on the face of TV display (Barco CCID 7751, Belgium) suitably linearized by gamma correction. To record transient VEPs, the spatial contrast was abruptly reversed at 1 Hz. To record steady-state responses the contrast was sinusoidally modulated at 1–15 Hz. The display (mean luminance 25 cd/m^2, area 24×26 cm) was placed 14 cm in front of the animal and centered on its midline, thereby covering $81 \times 86°$ of the visual field. Stimuli could be windowed to a vertical stripe of $10 \times 86°$ placed at different eccentricities in order to determine the visual field azimuth at which VEPs had their maximal amplitude. In some instances the stimulus pattern and window were rotated by 90° in order to determine the visual field elevation yielding maximal VEP amplitude.

2.3. Histology

At the end of the recording sessions the animals were transcardially perfused with saline solution followed with 4% paraformaldehyde in 0.1 M phosphate buffer

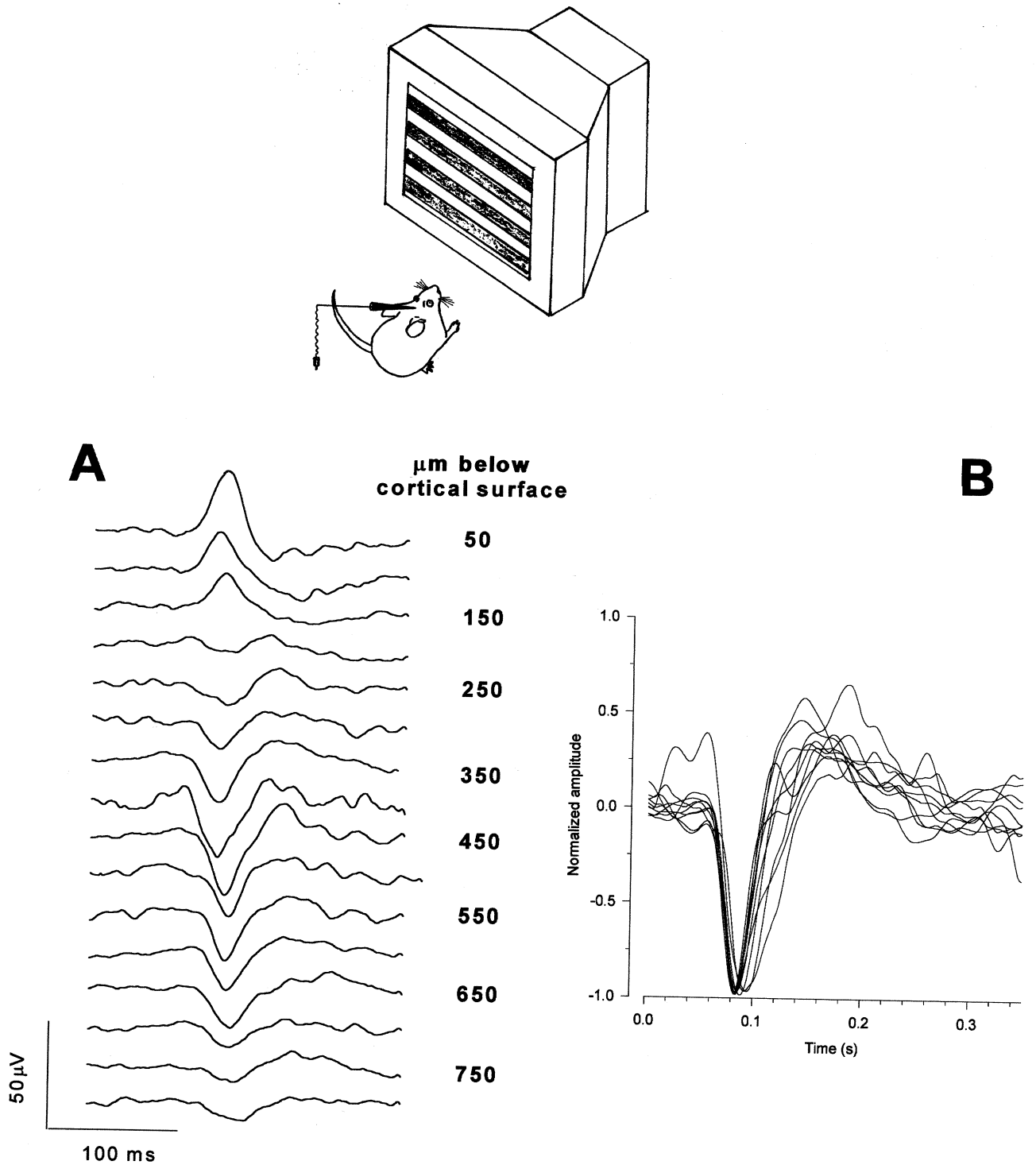

Fig. 1. Laminar analysis of the mouse VEPs. (A) Examples of VEPs recorded at different depths of the binocular visual cortex contralateral to the stimulated eye, in response to a visual pattern constituted of sinusoidal gratings (0.06 c/deg, 90% contrast, 25 cd/m^2 mean luminance, 81 × 86° field size, 1 Hz contrast reversal). The electrode was inserted 3.0 mm lateral to lambda. Note that the waveform reverses its polarity at about 200 µm cortical depth, suggesting a major dipole generator in layer II–III. (B) VEPs with maximal amplitude are recorded at 400 µm cortical depth, and display a major negative wave with a peak latency of 90–100 ms. Waveforms of different animals ($n = 10$) are superimposed to show consistency of contrast VEPs in mice.

at pH 7.4. The whole brain was removed and cryoprotected overnight with 30% sucrose. Sections of the visual cortex (40 μm) were cut with a freezing micro-tome, stained with cresyl violet (0.1%) dehydrated, covered and examined.

3. Results

3.1. Laminar analysis

Fig. 1 shows representative examples of transient VEPs recorded from the binocular cortex (contralateral to the stimulated eye) in response to a pattern of horizontal sinusoidal bars (0.06 c/deg spatial frequency, 90% contrast, field size $81 \times 86°$) whose spatial contrast is abruptly reversed at 1 Hz. The electrode has been inserted 3.0 mm lateral to the lambda. VEPs shown in Fig. 1A have been recorded in a single wild type mouse at different cortical depths. The VEP waveform is very simple, with a major component peaking at about 90–100 ms. In superficial layers (50–150 μm electrode advancement) the waveform is positive, whereas in deeper layers the waveform is negative. VEPs have their maximal amplitude at intermediate depths (around 400 μm electrode advancement). The VEP amplitude progressively decreases with further electrode advancement. This pattern of VEP depth profile is very consistent among animals. That the intracortical VEP profile shows a clear polarity inversion at a point between 150 and 200 μm electrode advancement suggests a major dipole source located at this cortical level. Anatomical reconstruction of electrode tracks indicates that the major dipole source is generated at the level of pyramidal cells in supragranular layers II–III.

Fig. 1B shows a series of VEPs recorded in different animals ($n = 10$) at the cortical depth at which responses have their largest amplitude (400 μm electrode advancement). Responses (normalized for amplitude) are superimposed to show that reproducibility of waveform and peak latency among animals is good. This kind of response has been chosen as the standard VEP to be used to evaluate visual performance, cortical retinotopy and ocularity.

3.2. Cortical retinotopy

Fig. 2 shows how VEPs have been used to evaluate cortical retinotopy. The visual stimulus has been windowed to a vertical stripe of 10° (see Section 2). For each electrode penetration, VEPs have been recorded at different window positions along the visual field azimuth (sketch in Fig. 2). Fig. 2A summarizes data obtained recording VEPs as a function of window position for series of evenly spaced electrode penetrations across the medio-lateral aspect of binocular cortex (2.2–3.0 mm lateral to lambda). It can be noted that for each electrode penetration there is a window position at which VEPs have a maximal amplitude. The VEP amplitude rapidly falls off for non optimal window positions. VEP data for each penetration have been fitted with a second-order polynomial, and the azimuth value corresponding to the peak in the function has been defined as VEP visual field azimuth, or VEP-VFA. As shown in Fig. 2B, the VEP-VFA shifts linearly with varying electrode position. The linear regression line fitting data points represents an index of the cortical magnification factor (degree of visual field/100 μm of cortical surface). In the example reported in Fig. 2A–B the cortical magnification factor is of the order of 7 deg/100 μm of cortical surface. The average magnification factor for comparable penetrations obtained in different mice ($n = 5$) was 6.6 deg/100

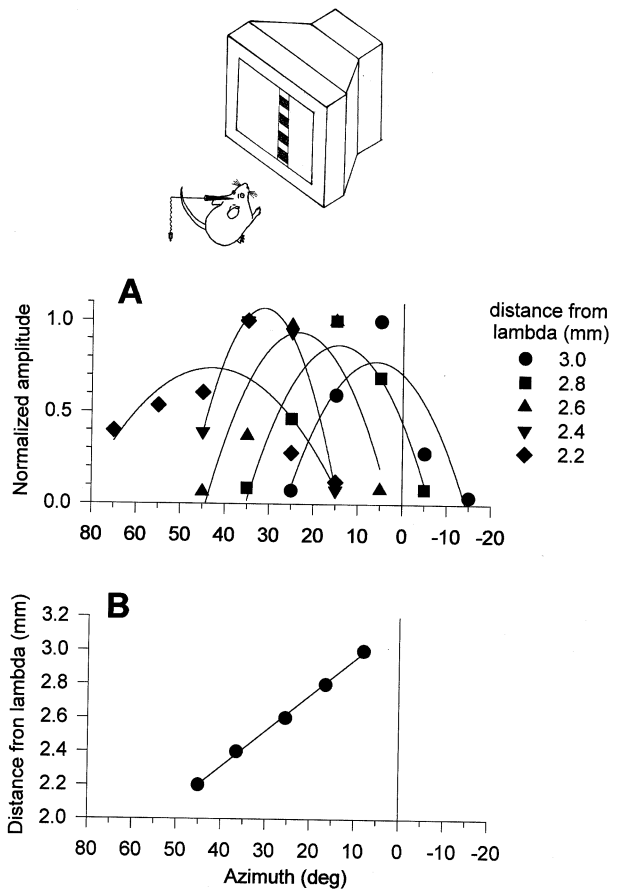

Fig. 2. Retinotopy of contrast VEPs. (A) The VEP visual field azimuth depends on electrode position over the medio-lateral aspect (2.2–3 mm from lambda) of the visual cortex. For each electrode placement, a series of VEPs were recorded as a function of the position of a windowed ($10 \times 86°$) stimulus along the horizontal meridian. VEP visual field azimuths were defined as the window position yielding maximal response amplitude. (B) The VEP visual field azimuth shifts linearly with electrode position. The slope of the regression line is a measure of the cortical magnification factor. In this representative example the cortical magnification factor is 7 deg/100 μm of cortex.

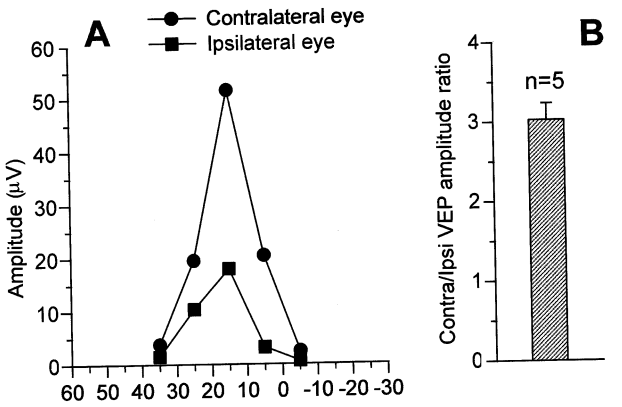

Fig. 3. Ocularity of contrast VEPs in mice. (A) Contrast VEPs can be recorded from either eye in response to a windowed ($10 \times 86°$) stimulus with different azimuths. Note that the VEP visual field azimuth (corresponding to maximal response amplitude) is about 15° from the vertical midline (0° azimuth) and is comparable in both eyes. However, VEPs in response to stimulation of the contralateral eye are about three times larger than those to stimulation of the ipsilateral eye. The recording electrode was inserted 3.0 mm lateral to lambda. (B) Average (+S.E.M.) contra/ipsi amplitude ratio obtained in a group ($n = 6$) of mice in response to an integrating stimulus.

μm (S.E.M. = 0.7). It is interesting that the magnification factor determined with VEPs is in a good agreement with that previously reported using extracellular recording of single units (Drager, 1975; Wagor et al., 1980; Gordon & Stryker, 1996; Hensch, Gordon, Brandon, McNight, Idzerda & Strycker, 1998). The main interest of this set of experiments was that of using VEPs to establish, in all animals tested, a cortical location from which record responses originating from the same region of the visual field (about 10 deg lateral to the vertical midline). In adult wild type mice this corresponded to 3.0 ± 0.05 mm lateral to lambda, on average. This cortical location agrees well with those previously reported using single unit recording (Drager, 1975; Wagor et al., 1980; Gordon & Stryker, 1996; Hensch et al., 1998). In three mice the stimulus and the window have been rotated by 90° to establish the window elevation yielding maximal VEPs when the electrode is located 3.0 mm lateral to lambda. This occurred when the window was centered 12–18° above the horizontal meridian, in agreement with Drager (1975) (not shown in figures).

3.3. Ocularity

Due to the predominance of crossed fibers in mouse retinal projections (Valverde, 1968; Grafstein, 1971; Drager & Olsen, 1980) the ocular dominance distribution of single units in the binocular visual cortex is strongly biased towards the contralateral eye (Drager, 1975, 1978; Gordon & Stryker, 1996; Hensch et al., 1998). We asked the question of whether it would be possible to use VEPs to have a reliable index of contralateral ocular bias. Fig. 3A shows one representative example of VEPs recorded from either eye as a function of the vertical window position along the visual field azimuth. The electrode was inserted 2.9 mm lateral to lambda and advanced 400 μm within the cortex. For both contra- and ipsilateral-eye stimulation, maximal VEP amplitude occurs at about 15° eccentricity. This confirms that eyes of anesthetized mice do not significantly diverge (Drager, 1975; Mangini & Pearlman, 1980; Gordon, Cioffi, Silva & Striker, 1996). Overall, the amplitude of VEPs of the contralateral eye is larger than that of the ipsilateral eye. There are several ways to evaluate the contralateral/ipsilateral VEP amplitude ratio; (1) between responses to optimally-presented windows (i.e. peak amplitudes); (2) between integrated responses (i.e. area subtended by each curve); (3) between responses to an integrating stimulus (i.e. a stimulus field larger than the region of visual field yielding significant VEPs). The amplitude of VEPs obtained in this latter way is slightly larger (about 20%) than that of VEPs in response to an optimally-presented window of 10°. This is because the spatial integration of the microelectrode is relatively small (see Section 2). In the example depicted in Fig. 3A, all approaches give a similar contralateral/ipsilateral VEP amplitude ratio of about 2.9. In order to simplify the procedure and reduce variability, we have chosen the solution of using an integrating full-field stimulus ($81 \times 86°$) and record a series of responses (at least ten) from each eye alternatively, whose average amplitude was used to evaluate the contralateral/ipsilateral VEP amplitude ratio. As shown in Fig. 3B, the contralateral/ipsilateral amplitude ratio was 3.0 on average ($n = 5$, S.E.M. = 0.2).

3.4. VEP acuity

One well established use of VEPs is to link cortical electrophysiology to sensory perception (Regan, 1989). In mice, the VEP approach has been limited to the use of diffuse flash stimuli to evaluate strain differences in light sensitivity (e.g. Green, Herrerose de Tejada & Glover, 1994). In this study we have exploited the possibilities offered by patterned stimuli to evaluate several aspects of spatio-temporal processing. Fig. 4 A–B shows how VEPs have been used to evaluate cortical spatial resolution (acuity). Responses were typically recorded from one microelectrode inserted 3.0 mm lateral to lambda and advanced 400 μm within the cortex in response to a full-field stimulus constituted of a horizontal grating of 90% contrast. Fig. 4A displays examples of responses recorded in one animal to stimuli of increasing spatial frequencies. As described for Fig. 1, at a spatial frequency of 0.06 c/deg VEPs display a major negative wave with a peak latency of 90–100 ms. By progressively increasing the stimulus spatial frequency, VEPs decrease in amplitude and increase in latency. Responses larger than noise can be measured up to 0.5 c/deg. Fig. 4B shows VEP amplitude data as

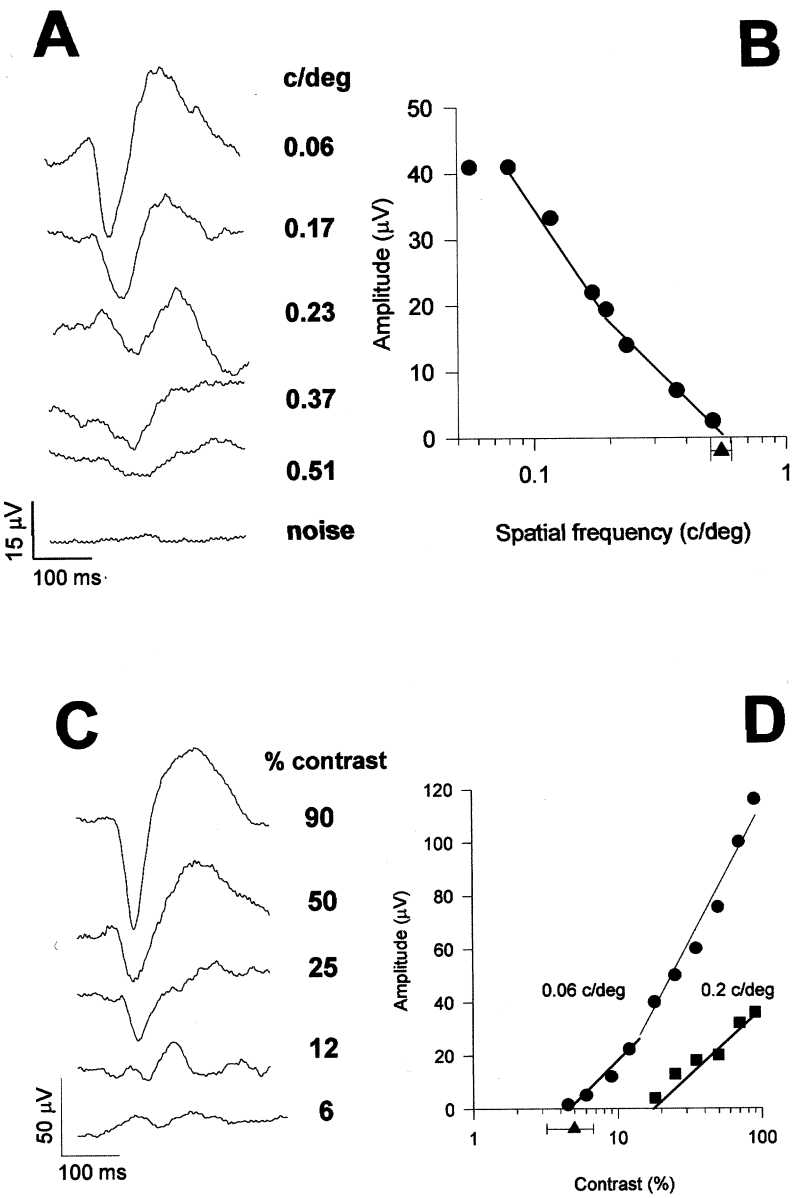

Fig. 4. Visual acuity and contrast sensitivity in the mouse. (A) Representative examples of VEPs in response to gratings of different spatial frequency (numbers to the right of tracings). With increasing spatial frequency, VEPs decrease in amplitude and increase in latency. At 0.5 c/deg spatial frequency, VEPs are barely distinguishable from a response to a blank field (noise). (B) Visual acuity is evaluated by extrapolating VEP amplitude data 0 V. The filled triangle below abscissa represents the average acuity (± S.E.M.) of a group ($n = 10$) of mice. (C) Representative examples of VEPs in response to gratings of 0.06 c/deg with different contrast (numbers to the right of tracings). VEPs progressively decrease in amplitude with decreasing contrast. Responses larger than noise can be recorded at 6% contrast. (D) Contrast threshold is obtained by extrapolating amplitude data to 0 V. Note that the contrast threshold is much lower at low (0.06 c/deg), as compared to higher (0.2 c/deg) spatial frequency. The filled triangle below abscissa represents the average contrast threshold (± S.E.M.) for 0.06 c/deg stimuli of a group ($n = 10$) of mice.

a function of log spatial frequency. Between 0.06 and 0.1 c/deg the VEP amplitude has an approximately constant value. Beyond 0.1 c/deg there is steep fall off in VEP amplitude. Acuity has been evaluated by linear extrapolation (semi-log coordinates) to 0 V of the set of data points close to the noise level as previously described for the rat (Pizzorusso, Fagiolini, Porciatti & Maffei, 1996). The average acuity found in different animals (filled triangle below the abscissa, $n = 10$) is of the order of 0.6 c/deg.

3.5. Contrast threshold

Fig. 4C displays examples of VEPs recorded in one mouse in response to a grating of 0.06 c/deg at different contrasts. With decreasing contrast, VEPs decrease pro-

gressively in amplitude and tend to increase in latency. Amplitude data for two different spatial frequencies as a function of log contrast are shown in Fig. 4D. As for Fig. 4B, threshold has been evaluated by linear extrapolation (semi-log coordinates) to 0 V of the set of data points close to the noise level. It can be noted that the contrast threshold depends on spatial frequency. At 0.06 c/deg the contrast threshold is of the order of 4.5%, whereas at 0.2 c/deg is much higher (about 17%). Contrast threshold has been evaluated in different ($n=10$) animals for stimuli of 0.06 c/deg (in the plateau range), and the average value (filled triangle below abscissa) was about 5%. Lower spatial frequencies could not be tested due to the technical impossibility of including a sufficient number (at least three) of cycles in the stimulus. The contrast threshold has not been systematically evaluated in the high spatial frequency range due to the very steep decay of VEP amplitude beyond 0.1 c/deg.

3.6. Temporal function

Fig. 5 summarizes the dependence of VEP amplitude on temporal frequency. Stimuli were standard gratings modulated in counterphase sinusoidally, to generate steady-state responses. At all temporal frequencies tested, steady-state VEPs were typically dominated by the stimulus second harmonic, whose amplitude and phase were evaluated (e.g. Porciatti, Burr, Morrone & Fiorentini, 1992). As shown in Fig. 5A, the VEP amplitude (second harmonic) is maximal at 2–5 Hz, and then progressively decreases with increasing temporal frequency. The temporal frequency cutoff is of the order of 12 Hz, similarly to that reported for rats using comparable experimental conditions (Pizzorusso et al., 1996). For temporal frequencies lower than 2 Hz there is a steep attenuation of the response. The second harmonic phase (Fig. 5B) progressively lags with increasing temporal frequency, showing a discontinuity at about 4 Hz. The phase characteristic were best fit with two different regression lines having different slopes (1–4 and 5–10 Hz). The slope of the phase characteristic (in π rad/Hz) divided by four (2nd harmonic*2 π rad) is an estimate of the latency (in seconds) of steady state responses (apparent latency: Regan, 1989). Apparent latencies in the range 5–10 and 1–4 Hz correspond to 110 and 192 ms, respectively, which are in the range of peak latencies of the major negative–positive waves of the transient responses shown in Fig. 1.

3.7. Motion sensitivity

We asked the question of whether reliable VEPs could be elicited by a stimulus set in motion, instead of contrast reversal of a static pattern. In four mice, VEPs have been recorded from the standard cortical location in response a stimulus constituted by horizontal sinusoidal bars (0.06 c/deg, 90% contrast, $98 \times 106°$ field) drifting vertically for 300 ms (motion onset) at different speeds (5–80 deg/s) and then stopping for 700 ms (motion offset). Fig. 6 summarizes the results of one experiment of this series. Comparable results have been obtained in other three mice. VEPs of significant amplitude can be generated for stimulus velocities higher that 5 deg/s (0.3 Hz). The waveform of motion VEPs is constituted by a major negative component at motion onset. Motion offset does not generate reliable responses. With increasing stimulus velocity, motion-onset VEPs increase in amplitude and shorten dramatically in latency. VEPs of maximal amplitude

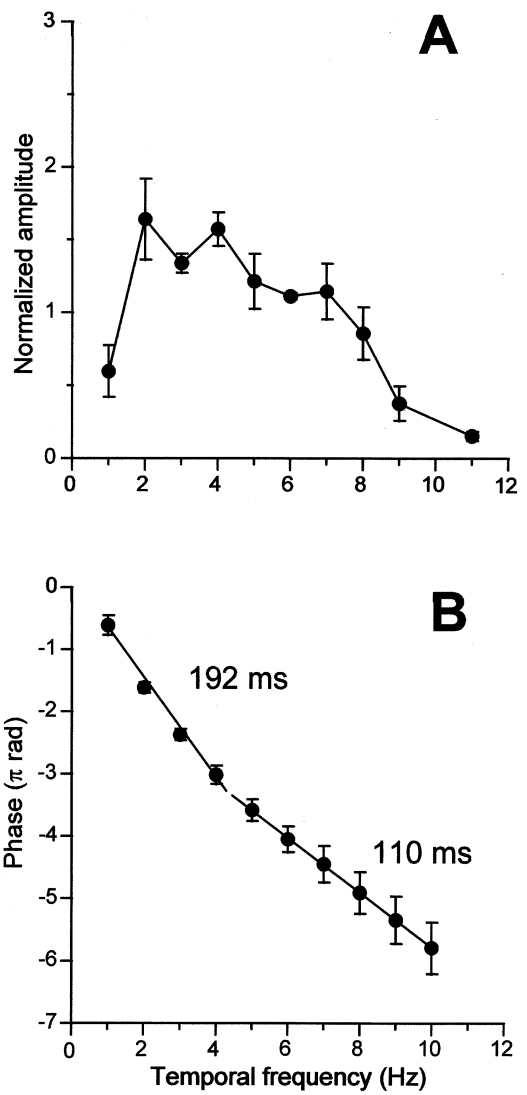

Fig. 5. Temporal function. Average ($\pm$S.E.M.) amplitude (A) and phase (B) of the VEP second harmonic as a function of temporal frequency, measured in a group of mice ($n=4$). The phase characteristic was fit with two regression lines for the frequency ranges 1–4 and 5–10 Hz, whose slopes were used to evaluate corresponding apparent latencies (numbers to the right of the curve). See Section 3 for further explanation.

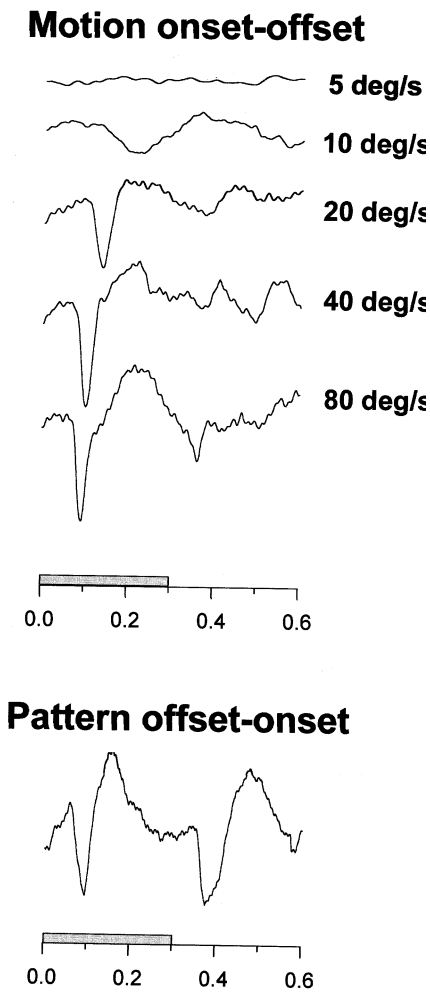

Fig. 6. Sensitivity to stimuli set in motion. Horizontal gratings of 0.06 c/deg set in motion for 300 ms evoke significant VEPs at velocities higher that 5 deg/s. The VEP amplitude increases, and latency decreases, with increasing stimulus velocity. For velocities higher than 80 deg/s, motion VEPs resemble those to static gratings presented in offset–onset mode.

and shortest latency (about 100 ms) are obtained at high stimulus velocity (80 deg/s: 4.8 Hz). With further increase of velocity another negative component becomes evident at motion offset with peak latency of about 400 ms (100 ms after stimulus offset). The waveform of motion onset–offset VEPs at highest velocities resembles that obtained in response to static stimuli presented in pattern offset–onset mode. This is in keeping with what has been previously suggested for humans: high velocity motion onset results in an abrupt reduction of contrast which elicits a pattern-offset VEP (Estevez & Spekreijse, 1974). The pattern becomes again suddenly visible at motion offset, thus eliciting a pattern-onset VEP. It is interesting that pattern-reversal, high velocity (80 deg/s) motion onset and pattern offset–onset responses all display virtually the same waveform, consisting of a negative wave peaking at about 100 ms. In addition, for all kind of VEPs the contrast dependence and contrast threshold are comparable (not shown in figures). This suggests similar cortical generators, sensitive to abrupt (high velocity) contrast changes in agreement with previous single-unit studies (Drager, 1975; Mangini & Pearlman, 1980).

3.8. Luminance dependence

The relationship between VEP amplitude (standard conditions) and mean luminance of stimulation is displayed in Fig. 7. The VEP amplitude is maximal at the highest luminance available (25 cd/m^2, low photopic range) and decreases progressively as luminance is reduced, to approach the noise level at 0.25 cd/m^2 (mesopic range). No response clearly above the noise level can be elicited in the scotopic range. Comparable results have been obtained in another animal. The strong photopic dependence of pattern VEPs indicates that responses are primarily cone-driven, similarly to primate VEPs (Regan, 1989). This may appear to some extent surprising, given that the mouse retina is about 97% rod-dominated (Carter-Dawson & LaVail, 1979). One should take into account, however, that the cone density in the mouse is about 12 000/mm^2 (Szel, Rohlich, Caffe, Juliusson, Aguirre & Van Veen, 1992) which is of the same order of the primate cone density at 4 mm retinal eccentricity. In addition, the density of cone bipolars is larger than that of rod bipolars by a factor of two (Strettoi & Masland, 1995; Ueda, Iwakabe, Masu, Suzuki & Nakanishi, 1997). Thus, the cone pathway appears sufficient to sustain robust cone-dominated pattern VEPs under conditions of light adaptation. Rod-dominated responses can be obtained in

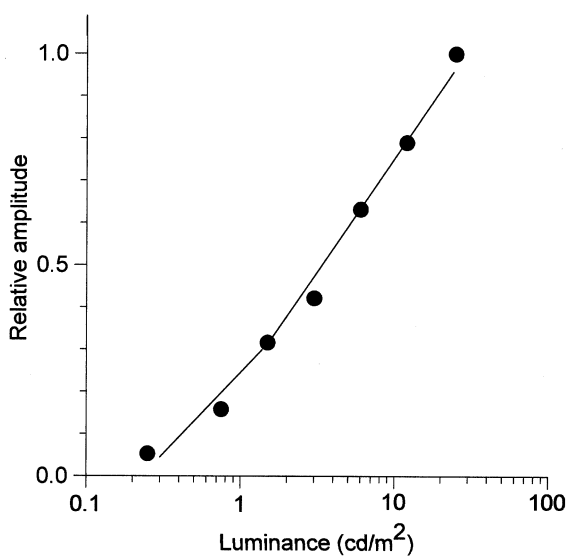

Fig. 7. Luminance dependence of contrast VEPs. The VEP amplitude increases monotonically with stimulus luminance over 2 log units in the mesopic to photopic range, suggesting that contrast VEPs are strongly cone-driven.

response to dim flashes of light under conditions of dark adaptation down to the absolute threshold (Green et al., 1994), which corresponds to the mouse behavioral visual sensitivity to light (Hayes & Balkema, 1993).

4. Discussion

The mouse has recently become the most studied mammal to investigate the cellular and molecular mechanisms underlying development, plasticity and regeneration in the central nervous system. Since basic knowledge of mouse visual physiology is scanty, a primary intent of our work was to provide a set of normative data for mouse vision. We have used the technique of pattern VEPs, which may offer the opportunity to characterize the visual phenotype of mouse mutants in which behavioral estimates are difficult or impossible to obtain because of cognitive or motor impairment (Crawley & Paylor, 1997; Post & Weiss, 1997). In addition, VEPs are a necessary complement to behavioral measures to establish whether a poor visual behavior has a sensory component. A secondary aim was to obtain hints on local cortical processing (cortical retinotopy, laminar analysis) and ocularity. This may represent important information in neurological mutants or in animals manipulated for studies of developmental plasticity (Katz & Shatz, 1996) and degeneration/regeneration (Aguayo et al., 1991).

4.1. Spatio-temporal aspects of mouse visual system

As shown by our results, the mouse spatial resolution (acuity) is of the order of 0.6 c/deg. This value is in excellent agreement with previous behavioral data obtained by either optokinetic responses (Sinex et al., 1979) or a forced choice procedure (Gianfranceschi, Fiorentini & Maffei, 1999). A visual acuity of 0.6 c/deg is about 40% lower than the behavioral acuity of the rat (e.g. Wiesenfield & Branchek, 1976; Dean, 1990). No information is currently available on the mouse contrast sensitivity. Our data show that the peak contrast threshold is about 5%, which is similar to the behavioral peak contrast sensitivity (contrast threshold^{-1}) of rats (Birch & Jacobs, 1979). The peak spatial frequency of 0.06 c/deg (bars of about 8°) compares well with the average receptive field size of single units of the binocular cortex (Drager, 1975; Mangini & Pearlman, 1980; Gordon & Stryker, 1996). It is interesting that the mouse peak contrast sensitivity is of the same order as that of humans for eccentrically (5–15°) presented stimuli (Rovamo, Virsu & Nasanen, 1978; Pointer & Hess, 1989). This is in keeping with the notion that the anatomical and functional organization of the peripheral retina is basically similar in mammals (e.g. Wassle & Boycott, 1991).

The temporal properties of the visual system are well described by the temporal frequency function. The VEP temporal frequency function of the mouse is band-pass tuned, with a maximum at 2–4 Hz, a pronounced roll-off at lower frequencies and a high temporal frequency cut-off at about 12 Hz (24 contrast reversal/s). The mouse temporal resolution is similar to that reported for rats (Pizzorusso et al., 1996). Differently from rats, however, the mouse temporal function does not show a major peak at frequencies lower than 1 Hz. The different form of the temporal function of rats and mice is reflected in the different waveform of transient responses. The rat transient VEPs, in addition to the early negative–positive complex, display a long latency (600–700 ms) major positive wave (Pizzorusso et al., 1996). In the mouse, transient VEPs show the early complex only. The peak latencies of the negative-positive complex are in fairly good agreement with the apparent latencies evaluated from the phase characteristics (see Section 3).

A further temporal property is the sensitivity to stimuli set in motion. Our results indicate that slowly moving patterns are poor visual stimuli whereas fast moving patterns are adequate stimuli to elicit VEPs of highest amplitude and shortest latency. The similarity of transient VEPs to fast motion onset, pattern onset-offset and pattern reversal suggests that VEP generators are best driven by abrupt (high velocity) contrast changes, in agreement with the properties of single cortical units (Drager, 1975; Mangini & Pearlman, 1980). The preference for stimuli of high velocity may be due to the characteristic of the eye optics. In the mouse, due to the small axial length of the eye and the relatively large size of the lens (Remtulla & Hallet, 1985), retinal images of external objects are very small. This implies that, in order a retinal image shifts at a given speed, the velocity of a moving stimulus has to be relatively higher.

4.2. Sources of pattern VEPs in the mouse

Laminar analysis and anatomical reconstruction of electrode track indicated that pattern VEPs are generated by a major dipole source, which is localized at the level of pyramidal cells in supragranular layers II–III. This appears to be a general feature of VEPs in response to pattern-reversal in mammals, in that comparable polarity inversion of the major VEP component has been reported to occur in the in supragranular layers of visual cortex of rats (Fontanesi, Siciliano, Porciatti & Bagnoli, 1996; Pizzorusso et al., 1996) and monkeys (Schroeder, Tenke, Givre, Arezzo & Vaughan, 1991).

The strong luminance dependence of VEPs indicate that they are primarily photopic in nature, as in primates. Thus, in spite of the a rod-dominated (97%)

retina, the cone pathway appears suitable to sustain robust cortical responses. Cortical retinotopy using VEP-Visual Field Azimuths was evaluated for a mediolateral slice at the level of lambda, and was found to closely correspond to that previously reported by evaluating Receptive Field Centers of single cortical units (Drager, 1975; Wagor et al., 1980). The cortical magnification factor (degree of visual field/100 μm of cortex) also corresponded between VEP and single unit measurements. Assessing at least one slice of the retinotopic map in the cortex was a necessary step to record activity driven by a specific region of the visual field. VEPs recorded from a region of the primary visual cortex close to the representation of the vertical meridian showed different contribution of the two eyes. Responses driven from the contralateral eye were larger than those of the ipsilateral eye by a factor of about three on average. This VEP contralateral bias may appear somehow small, given that the great majority (97.4%) of retinal ganglion cells projects to the contralateral side of the brain (Drager & Olsen, 1980). However, it is known that the physiological strength of the ipsilateral input is greatly amplified as a result of the prevalence of thalamic, as compared to tectal, uncrossed projections (La Vail, Nixon & Sidman, 1978; Drager & Olsen, 1980; Balkema & Drager, 1990).

In summary, our results show that a number of basic properties of the mouse visual physiology can be evaluated by means of pattern VEP. This technique can be easily applied to study the effect of genetic manipulation in transgenic mice. For instance, we have recently shown that the development of VEP spatial resolution (visual acuity) is accelerated in mice with cortical over expression of Brain Derived Neurotrophic Factor (BDNF) (Huang, Kirkwood, Porciatti, Pizzorusso, Maffei & Tonegawa, 1998).

Acknowledgements

This work was partially supported by the Foundation International Research Institute for Paraplegia (Grant P24), by the EEC (Biotech grant BIO4-CT96-0774) and by the Telethon Foundation project # 934. The authors wish to thank Professor Adriana Fiorentini for helpful suggestions and critical comments on this manuscript.

References

Aguayo, A. J., Rasminsky, M., Bray, G. M., Carbonetto, S., McKerracher, L., Villegas-Perez, M. P., et al. (1991). Degenerative and regenerative responses of injured neurons in the central nervous system of adult mammals. *Philosophical Transaction of the Royal Society of London B*: *Biological Science*, *331*, 337–343.

Balkema, G. W., & Drager, U. C. (1990). Origins of uncrossed retinal projections in normal and hypopigmented mice. *Visual Neuroscience*, *4*, 595–604.

Birch, D., & Jacobs, G. H. (1979). Spatial contrast sensitivity in albino and pigmented rats. *Vision Research*, *19*, 933–937.

Carter-Dawson, L. D., & LaVail, M. M. (1979). Rods and cones in the mouse retina. I. Structural analysis using light and electron microscopy. *Journal of Comparative Neurology*, *188*, 245–262.

Crawley, J. N., & Paylor, R. (1997). A proposed test battery and constellations of specific behavioral paradigms to investigate the behavioral phenotypes of transgenic and knockout mice. *Hormones and Behaviour*, *31*, 197–211.

Dean, P. (1990). Sensory cortex: visual perceptual functions. In B. Kolb, & R. C. Tees, *The cerebral cortex of the rat* (pp. 275–307). Cambridge: MIT.

Drager, U. (1978). Observations on monocular deprivation in mice. *Journal of Neurophysiology*, *41*, 28–42.

Drager, U. C. (1975). Receptive fields of single cells and topography in mouse visual cortex. *Journal of Comparative Neurology*, *160*, 269–290.

Drager, U. C., & Olsen, J. F. (1980). Origins of crossed and uncrossed retinal projections in pigmented and albino mice. *Journal of Comparative Neurology*, *191*, 383–412.

Estevez, O., & Spekreijse, H. (1974). Relationship between pattern appearance-disappearance and pattern reversal response. *Experimental Brain Research*, *19*, 233–238.

Fontanesi, G., Siciliano, R., Porciatti, V., & Bagnoli, P. (1996). Somatostatin depletion modifies the functional activity of the visual cortex in the rat. *Visual Neuroscience*, *3*, 327–334.

Fraunfelder, F. T., & Burns, R. P. (1970). Acute reversible lens opacity: caused by drugs, cold, anoxia, asphyxia, stress, death and dehydration. *Experimental Eye Research*, *10*, 19–30.

Fuller, J. L., & Wimer, R. E. (1966). Neural, sensory, and motor functions. In E. L. Green, *Biology of the laboratory mouse*. New York: McGraw Hill.

Gianfranceschi, L., Fiorentini, A., & Maffei, L. (1999). Behavioural visual acuity of wild-type and Bcl-2 transgenic mouse. *Vision Research*, *39*, 569–574.

Gordon, J. A., Cioffi, D., Silva, A. J., & Striker, M. P. (1996). Deficient plasticity in the primary cortex of alpha-calcium/calmodulin-dependent protein kinase II mutant mice. *Neuron*, *17*, 491–499.

Gordon, J. A., & Stryker, M. P. (1996). Experience-dependent plasticity of binocular responses in the primary visual cortex of the mouse. *Journal of Neuroscience*, *16*, 3274–3286.

Grafstein, M. (1971). Transneuronal transfer of radioactivity in the central nervous system. *Science*, *172*, 177–179.

Green, D. G., Herrerose de Tejada, P., & Glover, M. J. (1994). Electrophysiological estimates of visual sensitivity in albino and pigmented mice. *Visual Neuroscience*, *11*, 919–925.

Hayes, J. M., & Balkema, G. W. (1993). Elevated dark-adapted threshold in hypopigmented mice measured with a water maze screening apparatus. *Behavior Genetics*, *23*, 395–403.

Hensch, T. K., Gordon, J. A., Brandon, E. P., McNight, G. S., Idzerda, R. L., & Strycker, M. P. (1998). Comparison of plasticity in vivo and in vitro in the developing visual cortex of normal and protein kinase A RIbeta-deficient mice. *Journal of Neuroscience*, *18*, 2108–2117.

Huang, Z. J., Kirkwood, A., Porciatti, V., Pizzorusso, T., Maffei, L., & Tonegawa, S. (1998). A precocious development of the visual cortex and visual acuity in transgenic mice overexpressing BDNF in the postnatal forebrain. *Society for Neuroscience Abstracts*, *24*, 1517.

Katz, L. C., & Shatz, C. J. (1996). Synaptic activity and the construction of cortical circuits. *Science*, *274*, 1133–1138.

La Vail, J. H., Nixon, R. A., & Sidman, R. L. (1978). Genetic control of retinal ganglion cell projection. *Journal of Comparative Neurology*, *182*, 399–422.

Mangini, N. J., & Pearlman, A. L. (1980). Laminar distribution of receptive field properties in the primary visual cortex of the mouse. *Journal of Comparative Neurology*, *193*, 203–222.

Pizzorusso, T., Fagiolini, M., Porciatti, V., & Maffei, L. (1996). Temporal aspects of contrast Visual Evoked Potentials in the pigmented rat: changes with dark rearing. *Vision Research*, *37*, 389–395.

Pizzorusso, T., Porciatti, V., Strettoi, E., & Maffei, L. (1997). The visual physiology of the mouse determined with VEPs. A comparison between wild type and Bcl-2 overexpressing mice. *Society for Neursocience Abstracts*, *23*, 82.

Pointer, J. S., & Hess, R. F. (1989). The contrast sensitivity gradient across the human visual field: with emphasis on the low spatial frequency range. *Vision Research*, *29*, 1133–1151.

Porciatti, V., Burr, D. C., Morrone, C., & Fiorentini, A. (1992). The effects of ageing on the pattern electroretinogram and visual evoked potential in humans. *Vision Research*, *32*, 1199–1209.

Porciatti, V., Pizzorusso, T., Cenni, M. C., & Maffei, L. (1996). The visual response of retinal ganglion cells is not altered by optic nerve transection in transgenic mice overexpressing Bcl-2. *Proceedings of the National Academy of Science USA*, *93*, 14955–14959.

Post, R. M., & Weiss, S. R. (1997). Emergent properties of neural systems: how focal molecular neurobiological alterations can affect behavior. *Developments in Psychopathology*, *9*, 907–929.

Regan, D. (1989). Human brain electrophysiology. In *Evoked potentials and evoked magnetic fields in science and medicine*. New York: Elsevier.

Remtulla, S., & Hallet, P. E. (1985). A schematic eye for the mouse, and comparisons with the rat. *Vision Research*, *25*, 21–31.

Rovamo, J., Virsu, V., & Nasanen, R. (1978). Cortical magnification factor predicts the photopic contrast sensitivity of peripheral vision. *Nature* (*London*), *271*, 54–56.

Schroeder, C. E., Tenke, C. E., Givre, S. J., Arezzo, J. C., & Vaughan Jr., H. G. (1991). Striate cortical contribution to the surface-recorded pattern-reversal VEP in the alert monkey. *Vision Research*, *31*, 1143–1157.

Silva, A. J., Simpson, E. M., Takahashi, J. S., Lipp, H.-P., Nakanishi, S., Wehner, J. M., et al. (1997). Mutant mice and neuroscience: recommendations concerning genetic background. *19*, 755–759.

Sinex, D. G., Burdette, L. J., & Pearlman, A. L. (1979). A psichophysical investigation of spatial vision in the normal and reeler mutant mouse. *Vision Research*, *19*, 853–858.

Strettoi, E., & Masland, R. H. (1995). The organization of the inner nuclear layer of the rabbit retina. *Journal of Neuroscience*, *15*, 875–888.

Szel, A., Rohlich, P., Caffe, A. R., Juliusson, B., Aguirre, G., & Van Veen, T. (1992). Unique topographic separation of two spectral classes of cones in the mouse retina. *Journal of Comparative Neurology*, *15*, 327–342.

Ueda, Y., Iwakabe, H., Masu, M., Suzuki, M., & Nakanishi, S. (1997). The mGLUR6 5′ upstream transgene sequence directs a cell-specific and developmentally regulated expression in retinal rod and ON-type cone bipolar cells. *Journal of Neuroscience*, *17*, 3014–3023.

Valverde, F. (1968). Structural changes in the area striata of the mouse after enucleation. *Experimental Brain Research*, *5*, 274–292.

Wagor, E., Mangini, N. J., & Pearlman, A. L. (1980). Retinotopic organization of striate and extrastriate visual cortex in the mouse. *Journal of Comparative Neurology*, *193*, 187–202.

Wassle, H., & Boycott, B. B. (1991). Functional architecture of the mammalian retina. *Physiological Reviews*, *71*, 447–480.

Wiesenfield, Z., & Branchek, T. (1976). Refractive state and visual acuity in the hooded rat. *Vision Research*, *16*, 823–827.